Scan-pattern and signal processing for microvasculature visualization with complex SD-OCT: tissue-motion artifacts robustness and decorrelation time – blood vessel characteristics

Lev A. Matveev[1,2,3]*, Vladimir Yu. Zaitsev[1,2,3], Grigory V. Gelikonov[1,2], Alexandr L. Matveyev[1,2], Alexander A. Moiseev[1], Sergey Yu. Ksenofontov[1], Valentin M. Gelikonov[1,2,3], Valentin Demidov[4], Alex Vitkin[2,4]

[1]Institute of Applied Physics Russian Academy of Sciences, Ulyanova Street 46, 603950 Nizhniy Novgorod, Russia

[2]Nizhny Novgorod State Medical Academy, Minin Square 10/1, 603005 Nizhny Novgorod, Russia

[3]Nizhny Novgorod State University, Gagarina Avenue 23, Nizhny Novgorod 603950, Russia

[4]University of Toronto and University Health Network, 610 University Ave., Toronto, Ontario, M5G 2M9, Canada

ABSTRACT

We propose a modification of OCT scanning pattern and corresponding signal processing for 3D visualizing blood microcirculation from complex-signal B-scans. We describe the scanning pattern modifications that increase the methods' robustness to bulk tissue motion artifacts, with speed up to several cm/s. Based on these modifications, OCT-based angiography becomes more realistic under practical measurement conditions. For these scan pattern, we apply novel signal processing to separate the blood vessels with different decorrelation times, by varying of effective temporal diversity of processed signals.

Keywords: optical coherence tomography, angiography, image processing, speckle variance, flow diagnostics

1. INTRODUCTION

During the last 5-6 years, for elastographic and angiographic imaging, features of speckle structure, in particular its variability in OCT scans has been used. Namely, for microvasculature visualization[1,2,3], as well as elastographic imaging[4,5], variability of speckle patterns due to motion of scatterers can be used. While for elastography this motion is produced by the tissue deformation[5-14], for microcirculation, the temporal variability of speckle structure is related to the motion of scatterers in the liquid (e.g., blood) due to both collective flow and Brownian motion of scatterers or in some cases the Brownian motion can even give strongly dominating contribution[7] (in compare with Doppler techniques). For mapping regions of speckle-texture variability, various methods can be used, in particular correlation processing[2,15-19] or speckle-variance (Sv) methods[3,20-25]. However, the common feature of these approaches is that they use comparison of entire B-scans obtained consequently in the same plane. The time of B-scan acquisition typically is 2-3 orders of magnitude larger than for acquisition of individual A-lines. For typical interval between B-scans is about tens of milliseconds, so that obtaining consequent sufficiently-well coincided B-scans for reliable distinction between the stable "solid" pixels and variable, faster decorrelating "liquid" pixels is significantly complicated by natural inevitable motions of living tissue. For example, usually in realizations of Sv approach, the typical decorelation times for the blood in vessels on the order 10^1-10^2 ms require obtaining 8-10 repeated B-scans in a stack[2,20] since the typical B-scan acquisition rate ranges from several tens to about a hundred Hz. However, with increasing the time between compared B-scans the processing becomes also stronger sensitive to low-frequency tissue motions (breathing, heart beating, etc.) Thus realization of such Sv-based methods is complicated by the necessity of stabilization of the inspected tissue and/or elimination of the clatter-motion artifacts in the image post-processing. Besides, in such images all strongly decorrelated speckles in the vasculature image look similar and do not retain information on decorrelation-time differences for

*lionnn52rus@mail.ru; phone 7 831 436-7293; fax 7 831 436-5976; iapras.ru

Saratov Fall Meeting 2014: Optical Technologies in Biophysics and Medicine XVI; Laser Physics and Photonics XVI; and Computational Biophysics, E. A. Genina, V. L. Derbov, K. V. Larin, D. E. Postnov, V. V. Tuchin, Eds., Proc. of SPIE Vol. 9448, 94481M · © 2015 SPIE · CCC code: 1605-7422/15/$18 · doi: 10.1117/12.2179246

different vessels.

Here, we describe an OCT-based method for 3D visualizing blood microcirculation by noncomparative processing individual complex signal B-scans in which A-scans are densely spaced, so that the horizontal step between the adjacent A-scans is significantly smaller than the optical-beam diameter. The proposed approach allows to

1. increase the methods' robustness to bulk tissue motion artifacts;
2. separate the blood vessels with different decorrelation times, by varying of effective temporal diversity of processed signals.

2. OCT BASED M-MODE-LIKE SPECKLE VARIABILITY (MMLSV) APPROACH IMAGING OF 3D MICROVASCULATURE. SCAN-PATTERN DESCRIPTION.

The basic idea is to significantly slow down the lateral scanning beam speed so that the horizontal step between the adjacent A-scans is significantly smaller than the optical-beam diameter and retain hundreds of A-scans strongly correlated. This leads to M-Mode like scan-pattern. Namely, for each OCT system lateral resolution sampling volume there are several hundreds of A-scans actually in the M-mode. Then these A-scans can be processing to obtain the speckle blinking rate in each individual resolution volume.

The main features of this scan-pattern are:

1. The individual B-scans are not overlapped or may be slightly overlapped;
2. The individual A-scans in each B-scan are highly overlapped;
3. Thus, each lateral B-scan composed of densely overlapped A-scans is acquired only once for further processing;
4. Minimal time gap between processed data - equals to time gap between A-scans, that allows to better compensate bulk tissue motions.

We used a home-built Fourier domain spectral OCT scanner with the central optical wavelength 1,32 μm, bandwidth of 106 nm and a rate of 20 kHz for spectral fringes (yielding 10 kHz rate of the formed full complex-valued A-scans). The axial and lateral resolutions of the system are 10 μm and 20 μm, respectively. The latter corresponds to the effective diameter of the beam D_{beam}. In the depth direction, the spectrometer array enables 256 pixels and the chosen number of B-scans for 3D scanning also equals 256.

The beam speed V_{beam} in fast lateral direction of the B-scans is constant for each B-scan but slow to provide hundreds of spatially overlapped sequentially acquired A-scans. This provides a lateral scan time of one resolution volume equals to

$$T_{dec}^{\max} \approx \frac{D_{beam}}{V_{beam}} \tag{1}$$

that corresponds to maximum ultimate speckle decorrelation time that can be observed under those scan-pattern and OCT system parameters. For further demonstrations we set this speed equals to 0.6 mm/s. This corresponds to the $T_{dec}^{\max} \approx 33$ ms. For 256 B-scans (each 2 mm in lateral direction) covering the 2 mm x 2 mm area it takes 853 sec (~14 min).

The minimum ultimate speckle decorrelation time that can be observed is determined only by the complex A-scan rate $F_{\text{OCT\_rate}}$ and correspond to

$$T_{dec}^{\min} \approx \frac{1}{F_{OCT\_rate}} \tag{2}$$

As it was noted above the full complex A-scans rate of our OCT system is equal to 10 kHz and the $T_{dec}^{\min} \approx 0.1$ ms.

By varying the threshold frequency of this high-pass filtering (that will be described in the next section), the regions with different degree of complex-speckle variability can be detected and thus, the vessels can be separated by its decorrelation time.

3. OCT BASED M-MODE-LIKE SPECKLE VARIABILITY (MMLSV) APPROACH IMAGING OF 3D MICROVASCULATURE. SIGNAL PROCESSING DESCRIPTION.

The signal processing includes three steps:

1. Compensation of translational motions in the axial direction using phase equalization algorithm[26]. Average phases of overlapped A-scans can be equalized cumulatively;
2. High pass filtering of B-scans in its fast lateral direction using square filter with varying threshold;
3. Resampling of the filtered oversampled dense B-scans down to the lateral OCT-resolution determined by the beam diameter. Thus, the proposed technique visualizes the microvasculature with the resolution equal to that of the OCT-system.

Step 1 includes the calculation of the average phase difference for each two complex adjacent A-scans using Kasai estimatior[7,28]. Moreover, each phase calculation for the next pair is adjusted for the value of the previous calculation.

Step 2 includes the direct and inverse Fourier transform of each B-scan in its lateral direction. The main feature of the step 2 is that for each B-scan several filtrations with different filtering thresholds are performed in parallel. Thus, for each B-scan, we have several different filtering results separated by the threshold of square filters that provide separation of the regions with different degree of complex-speckle variability. Filter threshold F_{th} determines the maximum observed speckle decorrelation time for this filtration as

$$T_{dec}^{\max\_observed} \approx \frac{1}{F_{th}} \tag{3}$$

As the result of thus parallel processing resulting microvasulature images can be compared. The appearance of the vessels can be detected according to the filtering threshold.

Step 3 needs to be performed to reduce the resulting image size, because it contains redundant information in lateral direction.

4. DEMONSTRATIONS

For demonstrations we have acquire several 3D OCT scans on BulbC wild-type mice using above described scan pattern in Section 2.

The real OCT images before and after filtering are presented on Figure 1(a) and Figure 1(b) correspondingly to demonstrate the essence of this approach. On the Figure 1(a) only the small fragment of the high density B-scan is presented. The effect of the conversion of the speckle temporal blinking to its spatial breakup is demonstrated. It is clearly seen that the widely prolonged speckle on the vessel (the vessel part of the image indicated by dashed circle) has much higher spatial frequencies in compare with surrounding speckles. The non-blinking speckles on the tissue (corresponds to non-vessel part of the image) are prolonged due to the M-mode like acquisition. After applying the high-pass filtering in lateral direction (described in step 2 of the Section 3) only blinking speckles corresponds to the filter threshold parameter are remains. This speckles has the blinking rate corresponds to the F_{th} or higher. To plot maximal intensity projections (MIP) images we choose the depth range located on Figure 1(b) between two white dashed lines (60 and 200 px correspondingly). This depth range is set in order to avoid the artifacts appeared on the tissue surface. The MIPs itself are presented on Figure 1(c) for six filter threshold parameters. MIPs has the size of 2 mm x 2 mm. It is important to note, that this is the same data processed with varying high pass filter parameter in very wide range. We vary this parameter from 640 Hz to ultimate for described scan-pattern 30 Hz (that corresponds to scanning time of the single resolution volume). It is clearly seen that more vessels are appear at reduction filtering threshold. As it is noted above, corresponding maximum decorrelation time of the vessels for each threshold can be obtained using equation (3). By comparing these cases the vessels can be separated by their decorrelation time based on its detected blinking rate.

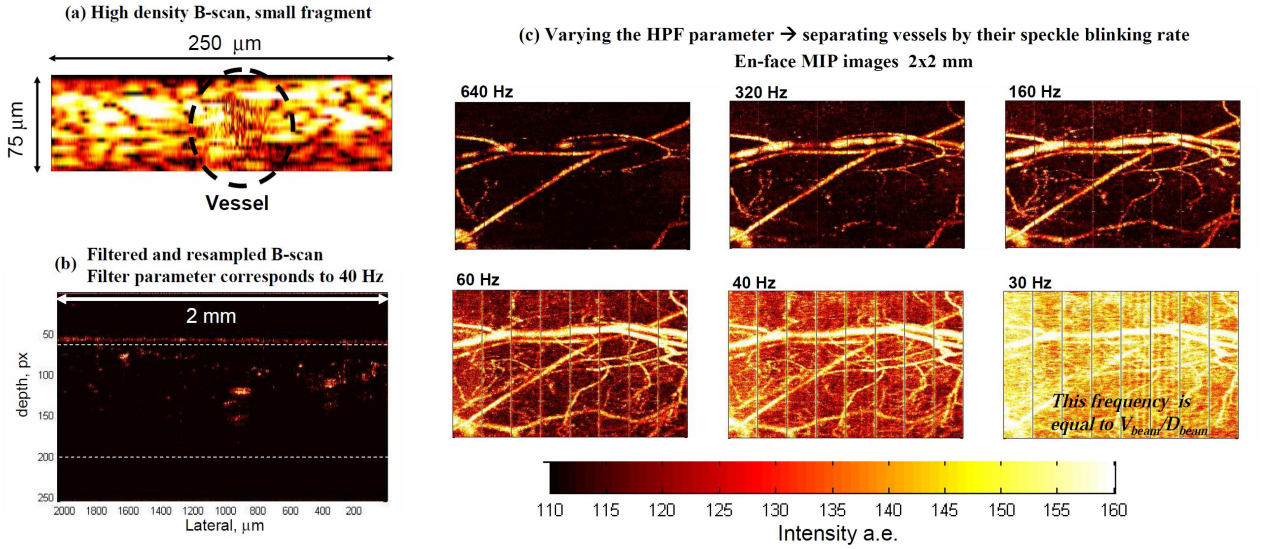

Figure 1. Panel (a) demonstrates the fragment of the B-scan with vessel. The speckles on the vessel are spatially distorted in compare to surroundings tissue. This distortion related to transformation of the speckle temporal blinking to its spatial distortion due to M-Mode like acquisition (slow scanning beam speed V_{beam}=0.6 mm/s). After applying the high pass filtering to suchwise formed 3D data set only distorted speckles are remained. The resulting B-scan after filtering is demonstrated on panel (b) for the high pass square filter threshold equals to 40 Hz. It means that only speckles with blinking rate from 40 Hz and higher are remained. By varying this filter threshold the vessels can be separated by its detected blinking rate. To detect its minimal speckle blinking rate panel (c) represents the six plots corresponds to the different filter threshold. The maximal decorrelation time corresponds to each case of filtering threshold can be estimated using equation (3). It is clearly seen from panel (c) that more vessels are appear at reduction filtering threshold.

5. DISCUSSION AND CONCLUSION

This ongoing research preliminary demonstrates the possibility of the vessel separation by its decorrelation time using conventional OCT technique. Moreover, the described M-Mode like approach provides the opportunity to separate the decorrelation time of the speckles in wide range. Namely, its ultimate range is between $T_{dec}^{\min}$ and $T_{dec}^{\max}$ (see eqs. (1) and (2)). For the used OCT system with scanning rate 10 kHz for full complex A-scans, lateral resolution of 20 µm and the chosen beam scanning speed V_{beam}=0.6 mm/s the ultimate separation range is possible between 0.1 ms and 33 ms. For more sophisticated patterns this range can be much wider (for example from 0.1 ms to 200 ms).

The reason for the difference in the speckle decorrelation time on the difference vessels is not yet clear. It can be supposed two possible reasons: flow itself (and difference in flow speed) and Brownian motions (and difference in its motion parameters). Basic estimations can be provided for both cases. We can assume two rough estimates:

1. Minimum velocity of mutual scatterer motion $V_{scatt} > (\lambda/4) * F_{th}$;
2. Minimum velocity of collective flow $V_{flow} > D_{beam} * F_{th}$.

For the vessels with speckle blinking rate from 640 Hz and higher these parameters are $V_{scatt} > 0.2$ mm/s and $V_{flow} > 13$ mm/s; for blinking rate 160 Hz and higher these parameters are $V_{scatt} > 0.05$ mm/s and $V_{flow} > 3$ mm/s; for blinking rate 40 Hz and higher - $V_{scatt} > 0.01$ mm/s and $V_{flow} > 0.8$ mm/s.

Despite the fact that they are in consistent with the possible actual values for both cases, it seems that further investigations are needed to separate this two cases (flows and Brownian motions).

All in all, proposed M-Mode like speckle variation approach to OCT based microangiography has several achievements:

1. Since the time gap between adjacent overlapped A-scans is much shorter than between B-scans, it is possible to compensate for artifacts of translational tissue motion (with speeds up to several cm/sec);

2. The High pass filtering uses both amplitude and phase information (whereas Doppler uses only phase and Sv/Cm methods uses only intensity), so it is not needed to combine the Doppler and Sv/Cm techniques in additional two-stage processing to obtain maximal information about vessels as it was made in recent publication[19];
3. The A-scans are compared (via filtering) not as individual pairs, but as groups of neighboring A-lines that provides better robustness and reduced information loss;
4. This allows the possibility to separate the vessels with different speckle blinking rates and different decorrelation time. In perspective it can be related to different scatterers motion/perturbation speed (eventually relate to important hemodynamic parameters such as flow speed and/or blood viscosity);
5. The same resolution in the angiographic image as in structural OCT images is ensured.

6. ACKNOWLEDGMENTS

Authors are grateful to Marina Sirotkina, Maria Karabut, Tatiana Pryanikova, Nataliya Buyanova and Anton Pavlikov (all from OCT Laboratory at the Nizhny Novgorod State Medical Academy, Nizhniy Novgorod, Russia) for their help during the experiments with the mice.

The authors acknowledge support of the Russian Federation Government contract No 14.B25.31.0015 for Leading Scientists to Russian Educational Institutions and the Russian Foundation of Basic Research (grants No 13-02-97131). VYZ and VMG acknowledge partial support by the contract No 02.B49.21.0003 between the Russian Ministry of Education and Nizhny Novgorod State University.

REFERENCES

[1] Mahmud, M. S., Cadotte, D. W., Vuong, B., Sun, C., Luk, T. W. H., Mariampillai, A., and Yang, V. X. D., "Review of speckle and phase variance optical coherence tomography to visualize microvascular networks," Journal of Biomedical Optics 18, 050901 (2013).
[2] Jonathan, E., Enfield, J., and Leahy, M. J. "Correlation mapping method for generating microcirculation morphology from optical coherence tomography (OCT) intensity images," Journal of Biophotonics 4(9), 583–587 (2011).
[3] Mariampillai, A., Standish, B. A., Moriyama, E. H., Khurana, M., Munce, N. R., Leung, M. K. K., Jiang, J., Cable, A., Wilson, B. C., Vitkin, I.A., and Yang, Y. X. D., "Speckle variance detection of microvasculature using swept-source optical coherence tomography," Optics Letters 33, 1530 (2008).
[4] Kennedy, B. F., Kennedy, K. M., and Sampson, D. D., "A review of optical coherence elastography: fundamentals, techniques and prospects," IEEE J. Sel. Topics Quantum Electron. 20, 7101217 (2014).
[5] Zaitsev, V. Yu., Matveev, L. A., Matveyev, A. L., Gelikonov, G. V., and Gelikonov, V. M., "Elastographic mapping in optical coherence tomography using an unconventional approach based on correlation stability," Journal of Biomedical Optics 19(2), 021107 (2014).
[6] Zaitsev, V. Y., Gelikonov, V. M., Matveev, L. A., Gelikonov, G. V., Matveyev, A. L., Shilyagin, P. A., and Vitkin, I. A., "Recent trends in multimodal optical coherence tomography . I . Polarization-sensitive oct and conventional approaches to OCT elastography," Radiophys. Quant. Electron. 57, 52 (2014).
[7] Zaitsev, V. Y., Vitkin, I. A., Matveev, L. A., Gelikonov, V. M., Matveyev, A. L., and Gelikonov, G. V., "Recent Trends in Multimodal Optical Coherence Tomography. II. The Correlation-Stability Approach in OCT Elastography and Methods for Visualization of Microcirculation," Radiophys. Quant. Electron. 57, 210 (2014).
[8] Matveev, L. A., Zaitsev, V. Y., Matveev, A. L., Gelikonov, G. V., Gelikonov, V. M., and Vitkin, A., "Novel methods for elasticity characterization using optical coherence tomography: Brief review and future prospects," Photonics & Lasers in Medicine 3(4), (2014) DOI: 10.1515/plm-2014-0023
[9] Zaitsev, V. Yu., Matveev, L. A., Gelikonov, G. V., Matveyev, A. L., and Gelikonov, V. M., "A correlation-stability approach to elasticity mapping in optical coherence tomography," Laser Physics Letters 10(6), 065601 (2013).
[10] Matveev, L. A., Zaitsev, V. Yu., Matveyev, A. L., Gelikonov, G. V., and Gelikonov, V. M., "Correlation-stability approach in optical microelastography of tissues," Proceedings of SPIE 8699, 869904 (2013).

[11] Zaitsev, V. Yu., Matveev, L. A., Matveyev, A. L., Gelikonov, G. V., and Gelikonov, V. M., "Correlation-stability elastography in OCT: algorithm and in vivo demonstrations," Proceedings of SPIE 8802, 880208 (2013).
[12] Matveev, L. A., Zaitsev, V. Yu., Matveyev, A. L., Gelikonov, G. V., and Gelikonov, V. M., "To the problem of stiffness-contrast quantification in the correlation-stability approach to OCT elastography," Proceedings of SPIE 9031, 903102 (2014).
[13] Zaitsev, V. Yu., Matveev, L. A., Gelikonov, G. V., Matveyev, A. L., and Gelikonov, V. M., "Towards free-hand implementation of OCT elastography: displacement-based approaches versus correlation-stability ones," Proceedings of SPIE 9129, 91290J (2014).
[14] Matveev, L. A., Zaitsev, V. Y., Matveyev, A. L., Gelikonov, G. V., and Gelikonov, V. M., "Combining the correlation-stability approach to OCT elastography with the speckle-variance evaluation for quantifying the stiffness differences," Proceedings of SPIE 9129, 91290I (2014).
[15] Enfield, J., Jonathan, E., and Leahy, M., "In vivo imaging of the microcirculation of the volar forearm using correlation mapping optical coherence tomography (cmOCT)," Biomed. Opt. Express 2, 1184-1193 (2011).
[16] Zafar, H., Enfield, J., O'Connell, M. L., Ramsay, B., Lynch, M., and Leahy, M. J., "Assessment of psoriatic plaque in vivo with correlation mapping optical coherence tomography," Skin Research and Technology 20(2), 141-146 (2014).
[17] Subhash, H. M., and Leahy, M. J., "Microcirculation imaging based on full-range high-speed spectral domain correlation mapping optical coherence tomography," Journal of biomedical optics 19(2), 021103 (2014).
[18] McNamara, P. M., Subhash, H. M., and Leahy, M. J., "In vivo full-field en face correlation mapping optical coherence tomography," Journal of biomedical optics 18(12), 126008 (2013).
[19] Choi, W.J., Reif, R., Yousefi, S., and Wang, R.K., "Improved microcirculation imaging of human skin in vivo using optical microangiography with a correlation mapping mask," Journal of Biomedical Optics 19(3), 036010 (2014).
[20] Mariampillai, A., Leung, M. K. K., Jarvi, M., Standish, B. A., Lee, K. K. C., Wilson, B. C., Vitkin, I. A., and Yang, Y. X. D., "Optimized speckle variance OCT imaging of microvasculature," Optics Letters 35, 1257 (2010).
[21] Conroy, L., DaCosta, R., and Vitkin, I.A., "Quantifying tissue microvasculature with speckle variance optical coherence tomography," Optics Letters 37, 3180 (2012).
[22] Lee, K. K., Mariampillai, A., Yu, J. X., Cadotte, D. W., Wilson, B. C., Standish, B. A., and Yang, V. X., "Real-time speckle variance swept-source optical coherence tomography using a graphics processing unit," Biomedical optics express 3(7), 1557 (2012).
[23] Ullah, H., Davoudi, B., Mariampillai, A., Hussain, G., Ikram, M., and Vitkin, I. A., "Quantification of glucose levels in flowing blood using M-mode swept source optical coherence tomography," Laser Physics 22(4), 797 (2012).
[24] Davoudi, B., Morrison, M., Bizheva, K., Yang, Y. X. D., Dinniwell, R., Levin, W., Vitkin, I. A., "A novel optical coherence tomography platform for microvascular imaging and quantification: initial experience in late radiation toxicity patients," Journal of Biomedical Optics 18(7), 076008 (2013).
[25] Sudheendran, N., Syed, S. H., Dickinson, M. E., Larina, I. V., and Larin, K. V., "Speckle variance OCT imaging of the vasculature in live mammalian embryos," Laser Physics Letters 8(3), 247 (2011).
[26] Moiseev, A. A., Gelikonov, G. V., Terpelov, D. A., Shilyagin, P. A., and Gelikonov, V. M., "Digital refocusing for transverse resolution improvement in optical coherence tomography," Laser Phys. Lett. 9, 826 (2012).
[27] Moiseev, A. A., Gelikonov, G. V., Shilyagin, P. A., Terpelov, D. A., and Gelikonov, V. M., "Digital refocusing in optical coherence tomography," Proceedings of SPIE 8213, 82132C (2012).
[28] Kasai, C., Namekawa, K., Koyano, A., and Omoto, R., "Real-time two-dimensional blood flow imaging using an autocorrelation technique," IEEE Trans. Sonics Ultrasonics 32, 458 (1985).